NEOTECTONIC DEVELOPMENT OF WESTERN MONTANA

Petr V. Yakovlev, Kaleb C. Scarberry, and Michael C. Stickney

Montana Bureau of Mines and Geology, Butte, Montana

ABSTRACT

Western Montana contains numerous active faults and landforms that record seismic activity, but these neotectonic features are understudied. Quaternary faulting has been primarily attributed to Basin and Range style extension and deformation associated with the Yellowstone hotspot. Patterns of regional seismicity, fault strike directions, Global Navigation Satellite System (GNSS) velocities, and P–T axis orientations of earthquake focal mechanisms support this conclusion. Regional patterns of deformation recorded in geodetic observations indicate large-scale rotation in the western United States, and changes in the extension directions near the Yellowstone hotspot. However, geodetic data in western Montana are problematic because of their small magnitudes with respect to error, and possible overprints from viscous deformation in the lower crust in response to large magnitude earthquakes that occurred in the 20th century.

Paleoseismic investigations have focused on Quaternary faults in southwestern Montana, where fault slip rates locally exceed 1 mm/yr (0.04 in/yr). Extension in southwestern Montana is likely affected by the Yellowstone hotspot, which changes regional stresses and the thermal and density structure of the crust. Additional paleoseismic investigations have been performed east of Helena and near Flathead Lake in northwestern Montana. Most paleoseismic records in the State contain evidence of earthquake clustering, with long periods of slow slip rates and presumably low seismic potential, and shorter periods of high slip rates and high seismic potential. Most Quaternary faults in Montana still lack paleoseismic data, providing avenues and motivation for future work.

Low-relief surfaces, such as pediments, peneplains, fluvial terraces, and bajadas record past periods of deformation, erosion, and deposition. Although no systematic framework describing and interpreting these features exists at present, we review previous investigations of low-relief surfaces in Montana using a consistent terminology. We further propose that applying modern geomorphology and geochronology techniques, such as cosmogenic radionuclide dating, optically stimulated luminescence dating, numerical modeling, and geomorphic indices may elucidate the ages and formation methods of low-relief surfaces in Montana.

INTRODUCTION

Western Montana is located at the northeastern edge of the Cenozoic Basin and Range extensional province, and is characterized by numerous Tertiary normal faults with diverse orientations (e.g., Bartholomew and others, 2009a; Pardee, 1950; Reynolds, 1979; Stickney and Bartholomew, 1987; Vuke and others, 2007; Zoback and Zoback, 1980; fig. 1). The Yellowstone hotspot has modified Miocene to present deformation in southwestern Montana. Normal faults oblique to the dominant northeast–southwest trend of Basin and Range style extension in western Montana are likely related to the Yellowstone hotspot (e.g., Sears and others, 2009). Likewise, a parabolic-shaped zone of heightened seismicity was likely generated by topographic uplift and thermal weakening of the crust near the Snake River Plain as a consequence of magmatism and mantle flow associated with the Yellowstone hotspot (Anders and others, 1989; Nishimura, 2003; fig. 2). However, the ages and slip histories of most extensional faults in Montana are currently unknown or poorly understood (USGS, 2006), making it difficult to attribute individual faults to a specific tectonic process.

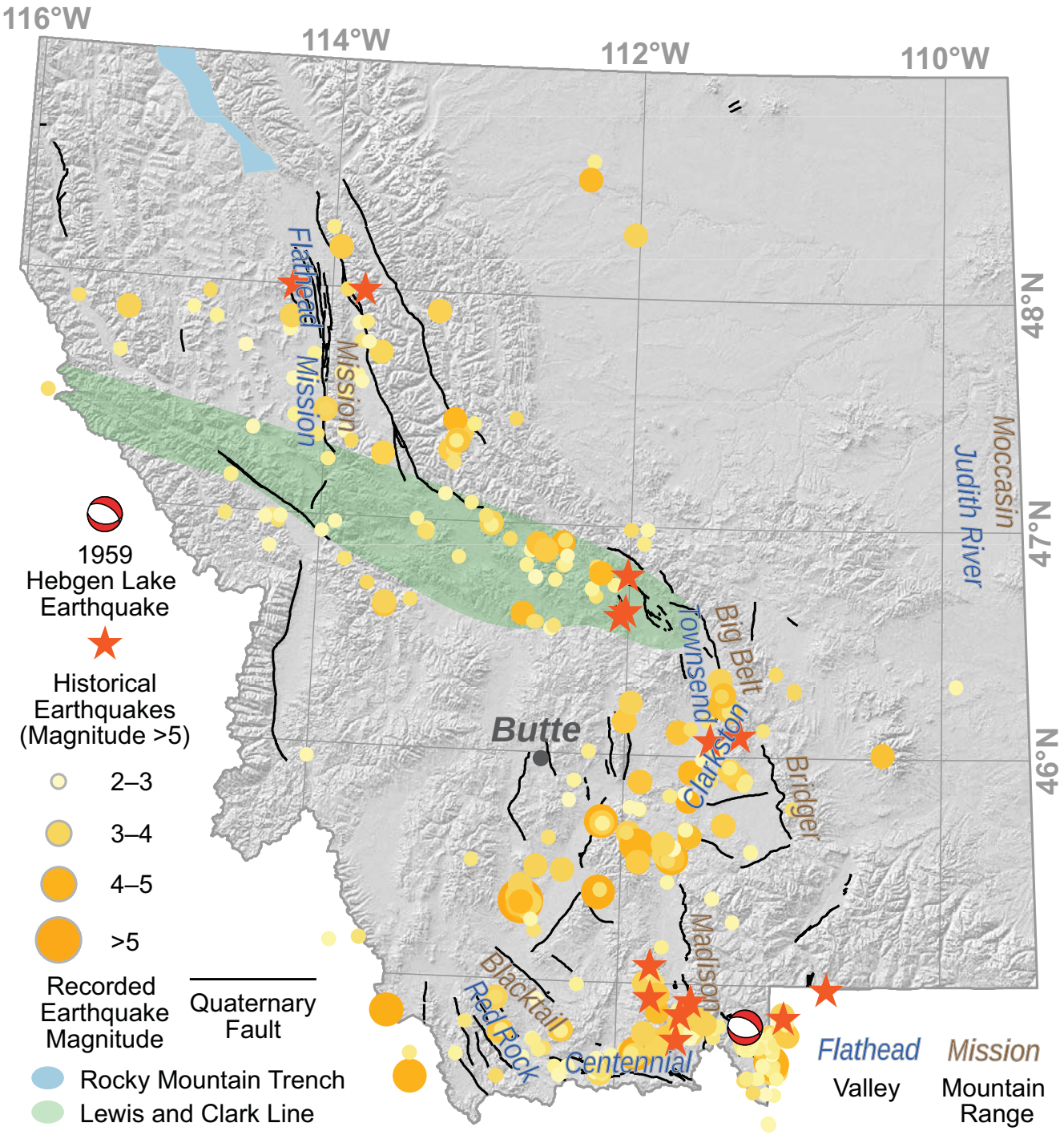

Figure 1. Quaternary faults, earthquakes, tectonic features, and topographic features of western Montana discussed in text. Insets show geography and fault names of regions discussed in detail. Centroid moment tensor for the 1959 Hebgen Lake earthquake from Doser (1985). Recorded earthquakes are from 1982-2017. Quaternary faults are from USGS (2006). Hillshade derived from Shuttle Radar Topography Mission (SRTM) elevation data (Farr and others, 2007).

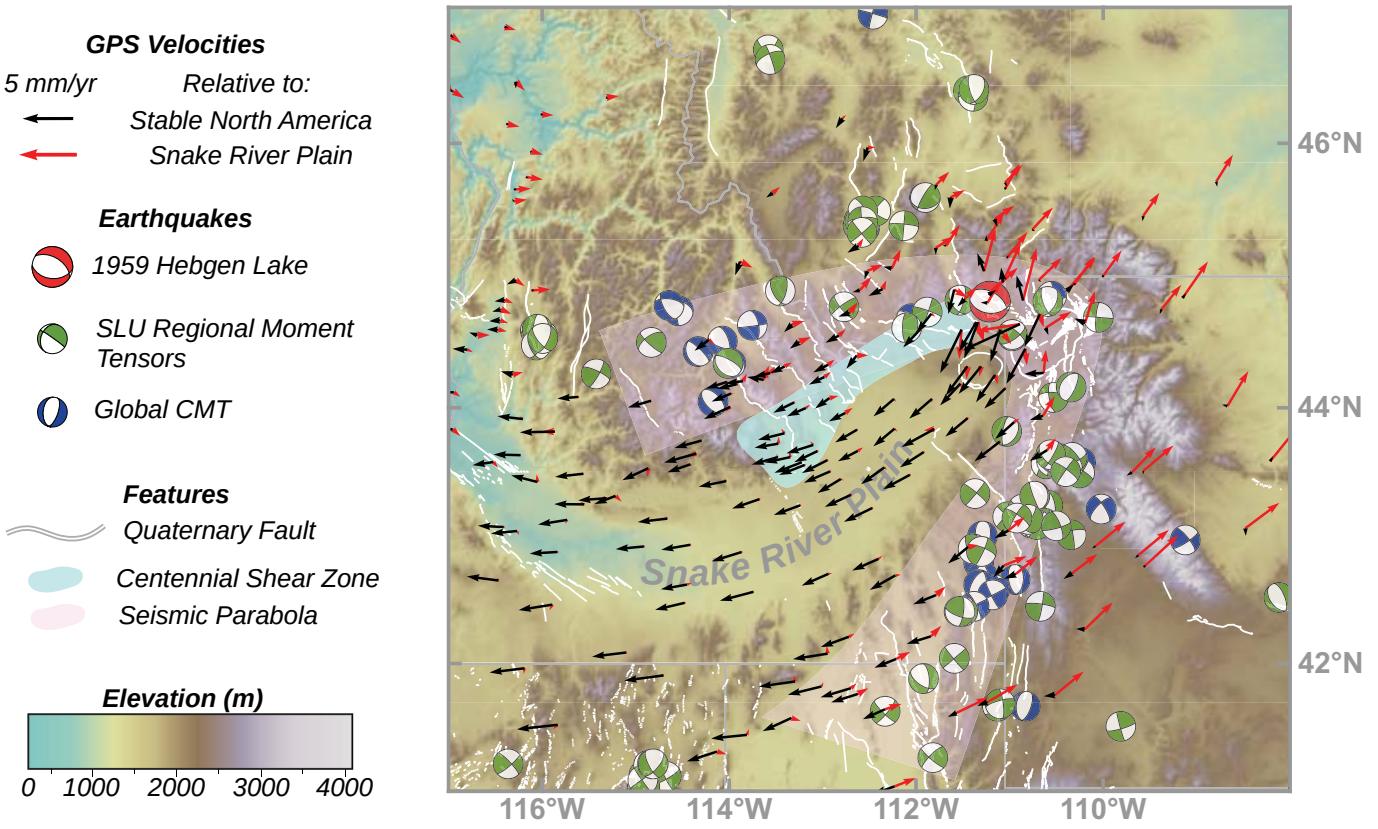

Figure 2. Geodetic velocities, earthquakes, tectonics features, and Quaternary faults near the Yellowstone hotspot. Black arrows show GNSS velocities with respect to a stable North America. Red arrows show GNSS velocities with respect to the Snake River Plain. Geodetic data from Schmeelk and others (2017). Red moment tensor is at location of the 1959 Hebgen Lake earthquake (Doser, 1985). Elevation data are from Shuttle Radar Topography Mission (SRTM) void filled data product (Farr and others, 2007). Blue moment tensor solutions are from the Global CMT catalog (Ekström and others, 2012). Green moment tensor solutions are from earthquakes in the St. Louis University moment tensor catalog with $\mathbf{M}_w$ >4. (Herrmann and others, 2011). Note velocities pointing away from the location of the 1959 Hebgen Lake earthquake in both reference frames, possibly due to short-term velocity changes induced by this earthquake (Nishimura, 2003; Schmeelk and others, 2017). Pink area shows approximate location of seismic parabola of Anders and others (1989).

Low-relief surfaces located at the tops of some mountain ranges and in intermontane valleys record the effects of fault movement, and have been interpreted as markers of Cenozoic changes in deformation and climate patterns (e.g., Alden, 1953; Atwood, 1916; Bevan, 1925). Recent advances in geochronology, geomorphology, and landscape evolution modeling have yet to be applied to landscapes in Montana, providing ample opportunity for future work. In this paper we summarize the current state of understanding of the neotectonic evolution of Montana, with a focus on the most rapidly deforming and best studied southwestern portion of the State. Limited information regarding slip rates and initiation ages of active faults or descriptions and chronology of low-relief surfaces outside of southwestern Montana is available at the time of writing.

REGIONAL KINEMATICS

Patterns of extension in western Montana have been variously incorporated or excluded from regional interpretations of deformation in the western United States (Brocher and others, 2017; Hofmann and others, 2006; Lageson and Stickney, 2000; Pardee, 1950). P–T axes of earthquakes in southwestern Montana indicate that the region accommodates deformation due to both northeast–southwest-directed Basin and Range style extension, and north–south extension attributed to the Yellowstone hotspot (Stickney and Bartholomew, 1987). However, if and how Montana fits into the Basin and Range extensional province, and how geodetic data may relate to regional patterns of deformation, remain enigmatic. Outstanding questions include: (1) How does faulting in western Montana fit into regional deformation patterns observed in geodetic studies and geologic syntheses (Brocher and

others, 2017; McCaffrey and others, 2013)? (2) What is the influence of the Yellowstone hotspot on the magnitudes and orientations of tensional stresses in southwestern Montana, and the spatial extent of this effect (Anders and others, 1989; Bartholomew and others, 2009a; Schmeelk and others, 2017)?

Geodetic Studies

Geodetic studies provide a first order constraint on contemporary regional patterns of deformation in the northwestern United States. Geodetic estimates of the short-term (years to decades) velocities of tectonic plates or crustal blocks are based on changes in the measured locations of specific sites on the Earth's surface. Positions of chosen sites are typically collected through the GNSS (Global Navigation Satellite System), either continuously by a dedicated antenna placed on the site, or at discrete intervals over multiple years (campaign style). The motion of faults, crustal blocks, and the flow of the mantle or lower crust, among other processes, may cause changes in the measured GNSS locations. These changes in GNSS locations are typically described as vectors split into horizontal and vertical components. Velocities are commonly described with respect to a reference continent, or crustal block, which is considered fixed in place for the purposes of geodetic analysis. Collection of GNSS velocities at multiple sites in a region generates a velocity field, representing block or plate motions.

Recent GNSS data show a broad regional pattern of clockwise rotation in the northwestern United States with respect to stable North America (McCaffrey and others, 2013; fig. 3). This pattern likely results from rotation of tectonic blocks in the Pacific Northwest and extension in the Basin and Range province,

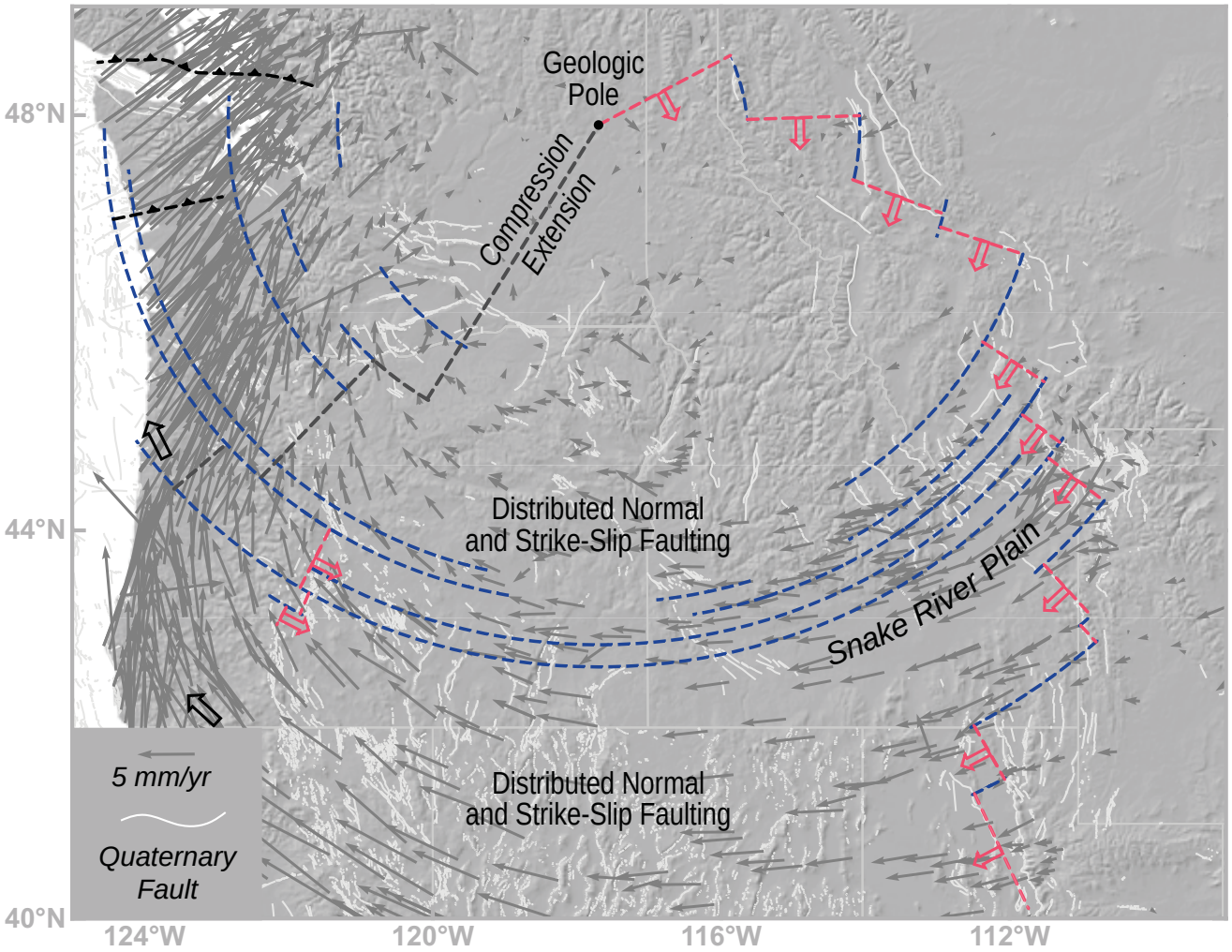

Figure 3. Tectonic setting of western Montana. Gray arrows are geodetic velocities with respect to stable North America (McCaffrey and others, 2013). White lines show known Quaternary faults (USGS, 2006). Light gray lines show state boundaries. Geologic pole of rotation and associated interpretations are from Brocher and others (2017). Dashed blue lines show equal velocity circles around the inferred geologic pole, with red lines showing possible strikes of extensional faults. Hillshade derived from Shuttle Radar Topography Mission (SRTM) elevation data (Farr and others, 2007).

including southwestern Montana, as part of the broader interaction between the Pacific and North American plates (McCaffrey and others, 2007, 2013). Regional fault patterns support a "geologic" pole of rotation for the northwestern United States located near the borders of Idaho and Washington, which is compatible with geodetic observations (Brocher and others, 2017; Kobayashi and others, 2016; fig. 3). However, patterns of regional rotation appear to break down in northwestern Montana, where velocities with respect to the stable North America are low (≤1 mm/yr), and typically have uncertainties comparable to recorded signals (McCaffrey and others, 2013; Payne and others, 2013). Regional rotation would imply north–south extension in northwestern Montana, but normal faults in the area strike north–south, indicating east–west extension (Vuke and others, 2007; fig. 1). Geodetic observations further imply that extension in western Montana should be balanced by ~0.7 mm/yr (~0.03 in/yr) of shortening along the Rocky Mountain Front (Schmeelk and others, 2017). However, tectonic studies show that shortening in the Rocky Mountain Front ended in Eocene time, and Quaternary shortening has not been observed in the area (Fuentes and others, 2011; Nemkin and others, 2016; USGS, 2006).

Short-term perturbations from large magnitude earthquakes may complicate geodetic data in western Montana. GNSS data typically contain short-term changes in magnitude and/or direction after large magnitude ($\mathbf{M}_w \geq 6.9$) earthquakes. Such short-term changes may be caused by aseismic creep along fault planes, and/or viscoelastic deformation of the lower crust or upper mantle after an earthquake (Deng, 1998; Pollitz and others, 2006; Wang and others, 2009). These perturbations typically decrease over time, as post-seismic strains are accommodated in the viscoelastic mantle or lower crust (e.g., Wang and others, 2009). Post-seismic changes in regional geodetic signals can last for up to a century (e.g., Vergnolle and others, 2003). In western Montana, post-seismic viscoelastic deformation may be localized in the lower crust (Nishimura, 2003). The short-term effects of the 1959 Hebgen Lake earthquake can be observed in modern geodetic data, as observed GNSS velocities point away from the earthquake epicenter (fig. 2). Observed geodetic velocities are consistent with a viscoelastic response of the lower crust to the Hebgen Lake earthquake, implying that perturbations to geodetic observations in Montana may last longer than the period of observation (Nishimura, 2003). Post-seismic changes in GNSS velocities from the viscoelastic relaxation of the lower crust in western Montana from the Hebgen Lake and the 1983 Borah Peak earthquakes are estimated to be up to 1 mm/yr, a magnitude similar to recorded geodetic signals (Nishimura, 2003; fig. 2).

Geodetic velocities record movements of up to 5 mm/yr (0.2 in/yr) near the Snake River Plain in southwestern Montana, compared to ≤1 mm/yr (≤0.04 in/yr) in the rest of the State (McCaffrey and others, 2013). Such changes in the magnitudes of geodetic velocities, as well as their directions, have been used to define the boundaries of tectonic features to the north of the Snake River Plain (e.g., Payne and others, 2013; fig. 2). Easterly directed geodetic velocities in southwestern Montana were used to argue that the region lies outside of the Basin and Range extensional province, where velocities are generally oriented towards the west (Schmeelk and others, 2017). However, this transition from easterly to westerly directed velocities is predicted by regional rotation (Brocher and others, 2017). Furthermore, geologic investigations place the northern boundary of the Basin and Range Province at the Lewis and Clark line of west-central Montana, ~200 km to the north of the Snake River Plain (Dickinson, 2006; McCaffrey and others, 2013; Reynolds, 1979; Sears and others, 2009; fig. 1). However the change in geodetic rates and directions north of the Snake River Plain is interpreted, geologic and geodetic observations equally support the existence of a zone of right lateral shear at the northern margin of the Snake River Plain, called the Centennial Shear Zone (Payne and others, 2008; fig. 2). Geodetic observations show that the Centennial Shear Zone accommodates 0.8–1.7 mm/yr (0.03–0.07 in/yr) of right lateral shear (Payne and others, 2008). Multiple high-angle conjugate strike-slip faults and distributed strain in regions between faults (Parker, 2016) accommodate this right lateral shear.

Effects of the Yellowstone Hotspot

Middle Miocene to present activity of the Yellowstone hotspot has produced a region of high topography, crustal weakness, heightened seismicity, and distinct patterns of normal faulting in southwestern Montana (e.g., Anders and others, 1989; Lowry and others, 2000; Sears and others, 2009). Beginning at 16 Ma, volcanism associated with the Yellowstone hotspot produced a sequence of calderas and volcanic fields that stretches from southeastern Oregon to northwestern Wyoming (e.g., Pierce and Morgan,

2009). This center of volcanism and related tectonic deformation have been propagating to the northeast at ~2.5 cm/yr (~0.2 in/yr) relative to stable North America since 10 Ma (Pierce and Morgan, 2009). Rhyolitic caldera eruption sequences along the Yellowstone hotspot track are overlain by 1–2 km (0.6–1.2 mi) of mantle-sourced basalt erupted from fissures, cinder cones, and small volcanoes (e.g., Shervais and others, 2006). These basaltic eruptions formed the low-relief topography of the Snake River Plain. Basaltic eruptions in the Snake River Plain were likely sourced from a 10-km-thick (6.2 mi) sequence of basaltic sills injected into the middle crust, which has been imaged by seismic receiver functions (Peng and Humphreys, 1998; Shervais and others, 2006).

Mantle flow associated with the Yellowstone hotspot creates a broad region of doming and increased surface elevations near Yellowstone, including a broad zone in southwest Montana. Surface uplift caused by mantle upwelling at the center of the Yellowstone hotspot in northwestern Wyoming is estimated to be as much as 2 km (1.2 mi; Becker and others, 2014; Lowry and others, 2000). However, the areal extent of this mantle-driven surface uplift, referred to as dynamic topography, remains uncertain. Numerical modeling of the Yellowstone hotspot plume implies an over 500 m (1,640 ft) increase in the surface elevations of southwestern Montana, with smaller topographic gains extending northward to the Canadian border (Lowry and others, 2000). This estimate for the magnitude and extent of dynamic topography uses an ~14 km (8.7 mi) effective elastic crustal thickness for much of western Montana that was inferred from topography and gravity data (Lowry and others, 2000). More recent geophysical investigations instead propose a 27 or 38 km (16.8 or 23.6 mi) effective elastic thickness of the crust in western Montana (Lowry and Pérez-Gussinyé, 2011; Nishimura, 2003). Higher effective elastic crustal thicknesses would imply that a smaller area of western Montana would be affected by dynamic topography generated by the Yellowstone hotspot than proposed by Lowry and others (2000). This inference is supported by analysis of data from the EarthScope USArray, which indicates that positive dynamic topography does not significantly extend past the Centennial and Madison Ranges of southwestern Montana (Becker and others, 2014; fig. 1). This conclusion is in agreement with geomorphic analyses, which show that dynamically supported topography extends ~200 km away from the Snake River Plain (Guerrero, 2017; Wegmann and others, 2007).

High topography surrounding the Snake River Plain, and magmatic intrusions beneath it, affect regional stresses and orientations of Quaternary extension. As the Yellowstone magmatic system has moved relative to North America since Miocene time, these stresses have overprinted older patterns of regional extension (Bartholomew and others, 2009b; Sears and others, 2009). A belt of heightened seismicity, commonly referred to as a "seismic parabola," is located near the high topography surrounding the Snake River Plain (Anders and others, 1989; fig. 2). Moment tensor solutions for earthquakes in southwest Montana have P–T axis orientations consistent with extensional stresses oriented in both the northeast–southwest and north–south directions. Although northeast–southwest extension is consistent with deformation associated with the Basin and Range extensional province, north–south extension is attributed to the Yellowstone hotspot (figs. 2, 3; Stickney and Bartholomew, 1987; Waite and Smith, 2004). South of the Yellowstone caldera, stress orientations inferred from earthquake focal mechanisms are deflected to the northeast from the dominant east–west trend associated with the Basin and Range in western Wyoming (Waite and Smith, 2004; White and others, 2009).

Changes in stress orientations and increased seismicity near the Snake River Plain may be generated by an increase in the gravitational potential of the crust, plate flexure, and changes in crustal strength caused by magma injection. High earthquake frequencies at the margins of the Snake River Plain may be driven in part by an increased gravitational potential of the crust caused by heightened elevations from dynamic topography (Pierce and Morgan, 2009). This inferred change in fault behavior because of topographic loading is consistent with recent work in the eastern Tibetan Plateau, which shows that topographic loads can change the stress states and dynamics of nearby faults (Styron and Hetland, 2015). High elevations at the margins of the Snake River Plain are in part caused by plate flexure driven by injection of ~10-km-thick (6.2 mi) mafic sill beneath the Snake River Plain (McQuarrie and Rodgers, 1998; Shervais and others, 2006). Crustal loading by this thick and dense intrusion brings the Snake River Plain to lower elevations, whereas plate flexure contributes to high elevations at its margins. Plate flexure is corroborated by increased plunges of major folds found at the margins of the

Snake River Plain towards its center, where they are overlain by basalt (McQuarrie and Rodgers, 1998). Plate flexure likely contributes to stress changes and heightened earthquake frequency at the margins of the Snake River Plain (Janecke and Blankenau, 2003; Pierce and Morgan, 2009; Waite and Smith, 2004; Zoback and Zoback, 1980). Thermal weakening of the crust outside of the Snake River Plain, and strengthening within it by basalt injection, may also lead to heightened seismicity (Anders and others, 1989).

Changes in stress orientations at the edge of the Snake River Plain then produce observed patterns of extension, where normal faults radiate from the Yellowstone hotspot track (e.g., Anders and others, 1989; Sears and others, 2009; Wegmann and others, 2007). Normal faults generated near the Yellowstone hotspot track have distinct orientations (e.g., the east–west-trending Centennial Range) and cut older normal faults associated with the Basin and Range Province (e.g., Anders and others, 1989; Sears and others, 2009). Recent studies propose that deformation at the margins of the Snake River Plain is not solely limited to normal faulting, and likely includes a strike-slip or oblique-slip component (Bartholomew and others, 2009a; Parker, 2016; Payne and others, 2013). Faults may accommodate extension associated with both the Yellowstone hotspot and the Basin and Range Province by switching slip directions between rupture events (Bartholomew and others, 2009a; Parker, 2016; Puskas and Smith, 2009).

TECTONIC GEOMORPHOLOGY

Geomorphic studies in western Montana describe diverse landscape features that formed as a consequence of both short term (kyr) and long-term (Myr) tectonic processes. Whereas fault scarps are key features associated with major fault systems in the region, we will discuss them in the following section. Here, we focus on long-lived low-relief surfaces that are pervasive throughout Montana, and their possible tectonic implications. Geomorphic studies in Montana generally use several terms for describing relict low-relief surfaces: peneplains, pediments, and fluvial terraces (fig. 4). These terms have explicit genetic implications, but are at times used interchangeably by different authors. An additional term, bajadas, is commonly a better fit for many of the surfaces described by existing work. All of these types of low-relief surfaces exist in Montana and formed on Myr to kyr timescales. A review of terms describing low-relief surfaces is thus required.

Peneplains, pediments, fluvial terraces, and bajadas are all low-relief surfaces that record prolonged periods of erosion or aggradation (fig. 4). Whereas in some locations these geomorphic features may appear similar, they differ markedly in their formation methods. Peneplains are regions of low relief thought to form by erosion of major mountain ranges to a specific base level (either the ocean or a closed basin). Peneplains may become heavily incised during subsequent periods of tectonic activity, producing broad disconnected low-relief surfaces at high elevation (Whipple and others, 2017). Pediments are gently sloping erosional surfaces formed on bedrock at mountain fronts (Hadley, 1967; Ritter and others, 2011). Usage of this term in Montana is often extended to include broad planar features formed by erosion of unconsolidated to poorly consolidated Tertiary basin deposits at mountain fronts (Atwood, 1916; Bevan, 1923; Reshkin, 1963). Pediments described in Montana are commonly covered by both fluvial and colluvial “gravel” deposits with clasts as large as boulder size (Atwood, 1916; Dresser, 1996; Schneider, 1994). Fluvial terraces are abandoned floodplains of streams or rivers that now lie at a higher elevation than the current streambed, which may have formed through either aggradation or erosion (Ritter and others, 2011). Bajadas are broad, low-relief depositional surfaces formed at mountain fronts by the merging of multiple alluvial fans (Ritter and others, 2011).

Early studies described the presence of multiple low-relief surfaces located above valley floors in Montana (e.g., Alden, 1932; Atwood, 1916). These low-relief surfaces were commonly interpreted to be peneplains that formed by beveling of topography to low relief at some point in the geologic past. Tectonic deformation and incision then brought these surfaces to high elevation relative to modern streams. After a century of work, however, there is no consensus on a systemic framework for describing these low-relief surfaces using modern terminology. Disagreements stem from three primary issues: (1) whether low-relief surfaces are true peneplains, rather than pediments, bajadas, or terraces; (2) correlation, or the lack thereof, of low-relief surfaces between valleys; and (3) the formation ages of individual low-relief surfaces.

Correlations of low-relief surfaces between valleys are typically based on surfaces at similar elevations, or having similar formation ages. Different slip rates on valley-bounding faults produced by Cenozoic

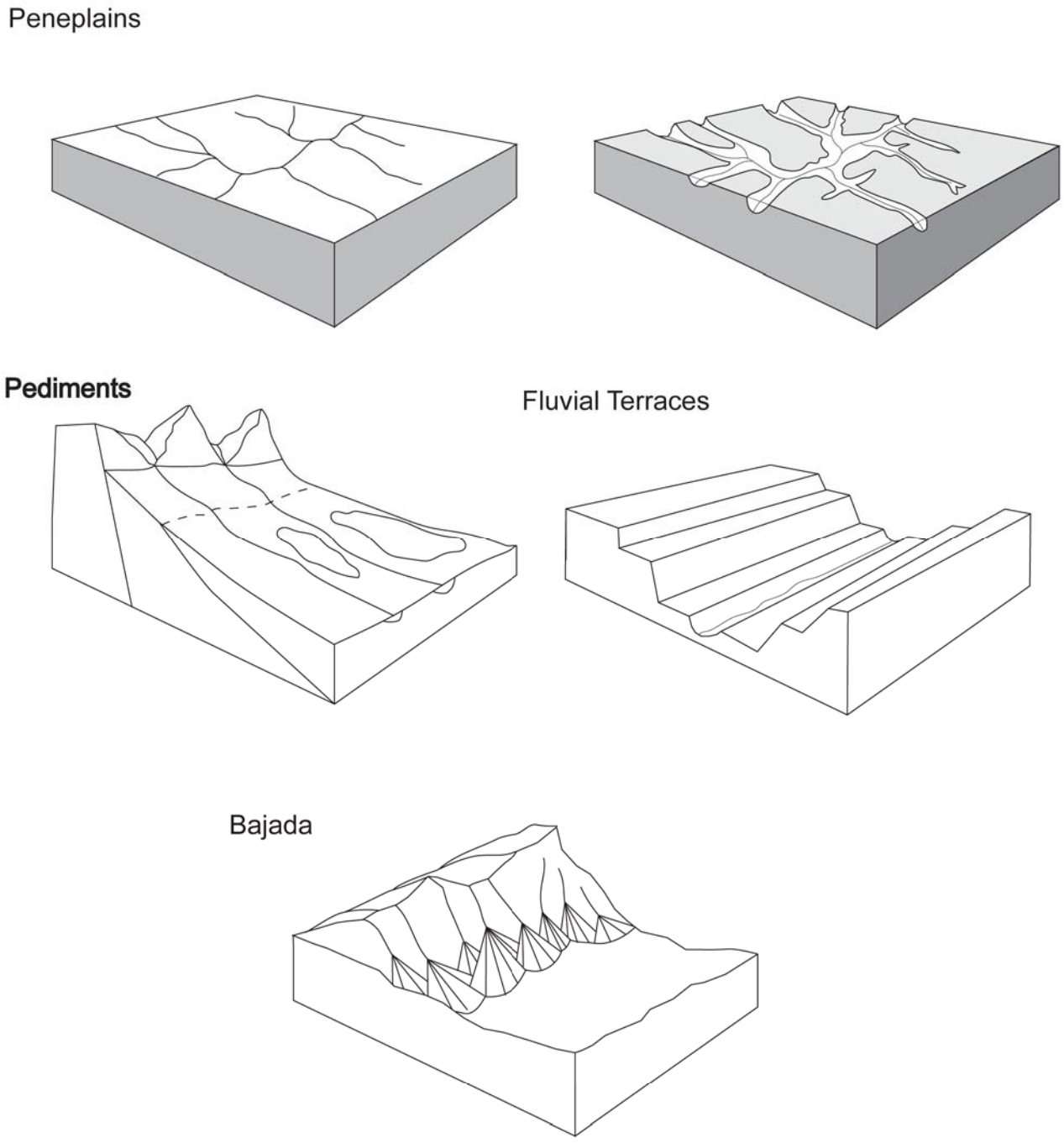

Figure 4. Types of low-relief surfaces common in Montana and discussed in this chapter.

extension would be expected to move low-relief surfaces formed at the same period of time to different elevations, making this style of correlation problematic. Formation ages of low-relief surfaces are largely constrained by stratigraphic correlations, and therefore rely on inferred ages of overlying or underlying strata. As modern radiometric techniques have provided new deposition ages for Tertiary and Quaternary deposits (e.g., Hanneman and others, 2003; Lindsey, 1982; Schwartz and others, 2019), inferred formation ages of low-relief surfaces may need to be revised. Consequentially, some surfaces once thought to be temporally correlative may have new stratigraphic constraints that would preclude correlation.

Regional Syntheses

Pardee (1950) synthesized observations of low-relief surfaces in western Montana, and proposed that in late Miocene time, western Montana was a broad region of low relief, or a peneplain. However, this synthesis includes all low-relief surfaces described in previous studies as peneplains, including probable pediments and terraces. A more systematic analysis of

low-relief surfaces in western Montana was performed by Alden (1953). Alden (1953) noted the presence of a complex system of low-relief surfaces in western Montana, with multiple surfaces of varying ages found in adjacent valleys. Alden (1953) described terraces and benches on both sides of the Continental Divide, and correlated these surfaces between intermontane basins, typically based on elevations above modern streambeds. He interpreted these surfaces as having formed during a period of continued uplift, with a cessation of uplift allowing for the formation of modern alluvial fans. Alden (1953) noted that gravels commonly covered benches and terraces in western Montana and interpreted some surfaces as remnants of old alluvial fan systems. These characteristics indicate that some surfaces described by Alden (1953) are actually pediments or bajada remnants (fig. 4). Alden (1953) grouped low-relief surfaces into three age brackets: (1) Pliocene to Pleistocene, (2) Early to middle Pleistocene, and (3) Late Pleistocene to Modern, which preclude the Eocene to Miocene ages for surfaces proposed by earlier authors (e.g., Atwood, 1916; Bevan, 1925). The formation age of the low-relief surfaces is based on stratigraphic position with respect to local glacial till deposits. The youngest surfaces are typically closest to modern stream levels, with older surfaces at higher elevations. However, surfaces vary in terms of both their absolute elevations and relative elevations above local stream levels between intermontane basins (e.g., Alden, 1932, 1953).

Identification and correlation of low-relief surfaces in western Montana (Alden, 1953) built upon work in eastern Montana (Alden, 1932), where low-relief surfaces formed by beveling of topography by ancient stream systems, and subsequent incision. Because these benches are often covered by fluvial gravels or glacial till, this mode of formation indicates that these low-relief surfaces can be described as pediments or peneplains (Lindsey, 1982; fig. 4). In the Judith River Basin (fig. 1), Alden (1932) interpreted the "Number 2 bench" as the remnant of an ancient system of alluvial fans, indicating that it can be classified as an ancient bajada. The three age groups of low-relief surfaces described by Alden (1953) were originally described by Alden (1932) in eastern Montana, and numbered as benches 1 to 3. However, the inferred ages of these surfaces are different from those identified in western Montana by Alden (1953). The Number 1 bench is the highest elevation surface with an inferred Miocene to Pliocene age. The Number 2 bench is a surface with intermediate elevations formed between 320 and 85 ka. The Number 3 bench is the youngest surface relative to stream levels that formed since 85 ka (Alden, 1932; Szabo and Lindsey, 1986).

The Flaxville Plain or Number 1 bench may be older than the highest elevation surfaces described in western Montana by Alden (1953). Fossil assemblages in the gravels that overlie the Flaxville Plain indicate a Miocene to Pliocene age for the surface, in contrast to the Pliocene to Pleistocene age of the highest benches described in western Montana (Szabo and Lindsey, 1986). Glacial deposits of early Pleistocene(?) age locally overlie the Number 1 bench, sparsely distributed and poorly preserved. Travertine that underlies the Number 2 surface in the Moccasin Mountains (fig. 1) developed after 320 kyr (Szabo and Lindsey, 1986). Till attributed to the Wisconsin glacial episode, the most recent advance of the Cordilleran Ice Sheet, locally overlies the Number 3 bench, indicating that it formed during the latest Pleistocene. The maximum age of the Number 3 bench, combined with the maximum age of the Number 2 bench in the Moccasin Mountains (fig. 1), implies that the Number 2 bench formed between 320 and 85 ka.

Additional studies investigating low-relief surfaces have been carried out near Butte, the Madison Valley, and the Beartooth Mountains. These are typically limited in their spatial extent, and commonly do not tie into the framework of Alden (1953). We describe them in detail in the following sections.

Butte, MT to the Madison Valley

Atwood (1916) described two peneplain levels near Butte: (1) A summit peneplain found 610–1,220 m (2,000–4,000 ft) above the valley floor, and (2) a sub-summit peneplain located ~90 m (~300 ft) above the valley floor. Erosion of the Boulder Batholith and Mesozoic sedimentary rocks formed the summit peneplain in Late Cretaceous to Eocene time, with subsequent deformation of and incision into the peneplain in Eocene to Oligocene time. The Late Cretaceous Boulder Batholith provides a maximum age for the summit peneplain. The Eocene lower Bozeman beds (now Bozeman Group) provide a minimum age for the formation of the summit peneplain, because they were deposited in valleys formed by incision of the summit peneplain (Atwood, 1916). The Bozeman beds are now assigned to the Eocene through earliest Miocene Renova Formation (Kuenzi and Fields, 1971; Fields and others, 1985), indicating that the summit pene-

plain formed between Late Cretaceous and Eocene time, if Atwood's (1916) stratigraphic correlations are correct. Pardee (1950) instead linked the summit peneplain to the top of the Bozeman beds and proposed that it had formed during a period of broad beveling and basin infilling in Eocene to Miocene time.

Atwood (1916) argued that the sub-summit peneplain near Butte formed in Eocene time, because basins containing the Bozeman beds became isolated and created a high-elevation base level. Streams then eroded down to this new, higher elevation base level, with the majority of erosion occurring in tributary streams and minimal erosion in upstream reaches. The sub-summit low-relief surface would be more correctly called a pediment rather than a peneplain, because Atwood (1916) does not describe the region being beveled to a low relief.

Reshkin (1963) identified a low-relief surface that lies between the valley floor and the summit peneplain to the east of the Continental Divide in the Jefferson Valley, at a similar position relative to the range front as the sub-summit peneplain of Atwood (1916). Because this low-relief surface cuts down at an increasingly shallow angle from the range front across both bedrock and Tertiary sediments, Reshkin identified it as a pediment. Reshkin noted that this surface was previously referred to as the Number 2 bench by Alden (1953), but locally renamed it the Vendome pediment. The Vendome pediment is locally covered by lag gravels. Reshkin mapped the Vendome pediment on both sides of the Jefferson River below the Elkhorn, Highland, and Tobacco Root Mountains, as well as the Ruby Range. Reshkin correlated the Vendome pediment to the Cameron bench of the Madison Valley, because the two surfaces merge on the bluffs between the Jefferson and Madison Rivers. The Cameron bench truncates a Bull Lake moraine and is overlain by a Pinedale moraine, indicating that it formed between the two glaciations (Reshkin, 1963). If the Vendome pediment and the sub-summit peneplain near Butte are indeed correlative with the Cameron bench, they must have also formed between the Bull Lake and Pinedale glaciations (130–30 kyr). The inferred 130–30 kyr age range for these surfaces is broadly correlative with the 320–85 kyr formation age for the Number 2 bench of Alden (1932) in eastern Montana (Szabo and Lindsey, 1986). More recent work concludes that the Cameron bench formed during a period of basin closure near the time of Bull Lake glaciation based on well-developed soils with a thick Bk horizon, indicating that it did not form coevally with the Vendome pediment (Schneider, 1994).

Beartooth Mountains and Absaroka Range

Bevan (1923) first described peneplains in the Beartooth Mountains northeast of Yellowstone National Park. He noted the presence of summit and lower elevation sub-summit peneplains in the range. Bevan inferred that the summit peneplain formed during a period of regional beveling that occurred after the end of regional deformation in early Oligocene time. He thus assigned the summit peneplain a Miocene or Pliocene in age, which would provide sufficient time for a regional lowering of relief and formation of a broad peneplain. Regional uplift and subsequent erosion then led to the formation of the sub-summit peneplain in Pliocene or Quaternary time (Bevan, 1923). These interpretations were later refined, based on a correlation with peneplains in the Absaroka Range and an Oligocene to Miocene age of sediments in the Gallatin Valley, which overlie the summit peneplain. The summit peneplain was then assigned an Oligocene age, and the sub-summit peneplain inferred to have formed in Pliocene time (Bevan, 1925).

A Cenozoic origin for the peneplains in the Beartooth Mountains is disputed by Simons and Armbrustmacher (1976). They note the presence of a regionally extensive Precambrian weathering surface, which was covered by Paleozoic rocks and subsequently deformed in Cretaceous to Tertiary time. They use geologic cross sections to link this weathering surface to the high-elevation peneplains in the Beartooth Mountains. Simons and Armbrustmacher (1976) conclude that Paleocene erosion of Paleozoic sedimentary rocks exposed this Precambrian weathering plain and produced the low-relief surfaces observed in modern time. Furthermore, Simons and Armbrustmacher (1976) infer that in the southeastern part of the range, the Precambrian weathering surface was likely exposed in Pliocene time after erosion of the Eocene Absaroka volcanic field. Glacial and fluvial erosion since Pliocene to Pleistocene time dissected the Precambrian erosional surface, producing steep valleys with the isolated flat-topped ranges observed today (Simons and Armbrustmacher, 1976).

Montagne and Chadwick (1982) note the presence of a prominent low-relief surface in the Absaroka Range, on the east side of the Yellowstone Valley in an

area referred to as the Short Hills. The surface is located 305 m (1,000 ft) above the valley surface, to the east of the west-dipping Deep Creek–Luccock normal fault. Although Montagne and Chadwick (1982) describe the surface as a pediment, they do not otherwise infer how it formed. Because the surface is overlain by sediments correlated with the middle Miocene to Pliocene Sixmile Creek Formation, Montagne and Chadwick (1982) infer that the pediment formed prior to middle Miocene time. The current position of the pediment above the modern valley floor may be caused by movement on the Deep Creek–Luccock normal fault, because the valley is dropped down relative to the Short Hills.

Current Views on Low-Relief Surfaces

The formation and development of low-relief surfaces commonly interpreted as peneplains are the subject of considerable recent debate. Like the examples described in Montana, many of these low-relief surfaces now lie at different elevations, are disconnected from one another, and are interpreted as having been formed by incision of an ancient peneplain. Yang and others (2015) proposed that low-relief surfaces can instead be generated by stream piracy and drainage capture driven by tectonic forcing. Therefore, low-relief surfaces need not be incised peneplains, and do not require regional erosion to a specific base level. As such, one needs to exercise caution in interpreting disconnected low-relief surfaces, as they may not represent past erosional conditions that beveled the region to low relief. Alternatively, Whipple and others (2017) proposed that disconnected low-relief surfaces may be generated by either drainage capture or incision of old peneplains. These authors propose a simple scheme for distinguishing between the two mechanisms for the formation of disconnected low-relief surfaces: (1) if formed by drainage capture, low-relief surfaces occur at varying elevations, have different average relief from one other, are bounded by drainage divides of affected tributaries, and are rimmed by high-relief topography; and (2) if formed by incision of peneplains, low-relief surfaces are instead located at similar elevations or elevations that lie on a stream gradient, are not bounded by drainage divides of local tributaries, and are not rimmed by high topography. These principles have not been applied to low-relief surfaces found in Montana, providing an opportunity for future investigations.

PALEOSEISMIC INVESTIGATIONS

Paleoseismic investigations in western Montana are limited, with most known Quaternary faults lacking crucial data on maximum credible earthquake magnitudes and earthquake recurrence intervals (Stickney and others, 2000; USGS, 2006). Regional seismic hazard assessments use data from less than a third of mapped Quaternary faults, which may lead to an underestimate of regional hazards (Petersen and others, 2014; Wong and others, 2005). Furthermore, the existence and connectivity extent between distinct fault segments is largely unknown. Fault segment interactions influence the maximum potential earthquakes possible on each individual fault as well as earthquake recurrence intervals (e.g., Crider and Pollard, 1998; Crone and Haller, 1991; Regalla and others, 2007). Recent geologic mapping provides evidence of heretofore unknown Quaternary structures that have yet to be added to Quaternary fault databases or incorporated in regional hazard assessments (e.g., Olson and others, 2016; Vuke and others, 2007). Here, we summarize the results of current paleoseismic investigations of Quaternary faults in western Montana.

Hebgen Basin and Southwestern Montana

The $\mathbf{M}_w$ 7.3 August 1959 Hebgen Lake earthquake is the largest recorded seismic event in Montana and has motivated abundant, although belated, paleoseismic investigations. Although the Hebgen Lake–Centennial–Madison Fault systems are some of the most discussed in Montana, the latter two faults have not yet been trenched. Faults in this region are characterized by abundant nearby seismicity and the highest fault slip rates in Montana, likely representing the largest seismic hazards in the State (Petersen and others, 2014). Faulting and seismicity in the region likely result from the combined effects of Basin and Range extension and the passage of the Yellowstone hotspot (Anders and others, 1989; Bartholomew and others, 2009b; Pierce and Morgan, 2009; Schmeelk and others, 2017; Stickney and Bartholomew, 1987).

The Hebgen Lake and Red Canyon Faults

The Hebgen Lake earthquake produced 29 km (18 mi) of fault scarps on two faults, the Hebgen Lake and Red Canyon Faults, along the north side of Hebgen Lake (fig. 1). These normal faults generally strike east–southeast and dip south. The Red Canyon Fault has an arcuate western section that varies by up to

120° in strike and a distinct east-striking, south-dipping segment. Fault scarps produced during the Hebgen Lake earthquake average 3 m (10 ft), but are locally as high as 6.7 m (20 ft; Witkind, 1964). Movement on the Red Canyon and Hebgen Lake Faults caused about 7 m (22 ft) of subsidence in Hebgen Lake, with an area covering ~1,552 km^2 (602 mi^2) experiencing measurable subsidence (Myers and Hamilton, 1964). The earthquake triggered multiple rock slides and landslides, the largest of which (the Madison slide) blocked the Madison River. The Madison slide was the biggest historical landslide in the northern Rockies (Doser, 1985; Hadley, 1964).

Paleoseismic investigations concluded that fault scarps along the Hebgen Lake and Red Canyon Faults recorded evidence of older earthquake events. A trench on the Red Canyon Fault showed that at least one other seismic event occurred on the fault since 15 ka. This older event produced a 2 m offset on a Quaternary surface with a cosmogenic radionuclide exposure age of 11–15 ka (Haller and others, 2002). ^{36}Cl cosmogenic radionuclide exposure dating of a bedrock fault scarp along the Hebgen Lake Fault yielded ages and magnitudes of major slip events along the fault from 37 ka to present. The highest slip rates on this fault scarp were estimated as occurring at 24–20 ka and 7–0 ka, indicating periods of earthquake clustering (Zreda and Noller, 1998). However, subsequent geomorphic and trenching investigations have found no evidence for the high number of events inferred from this bedrock scarp and record only one event prior to the 1959 rupture (Ruleman and others, 2014). This older rupture likely occurred since 6–10 ka, based on 6–10 ka surfaces offset by 2.2 m (7.2 ft) prior to the 1959 earthquake (Ruleman and others, 2014). Morphologic dating of faults at the south end of Hebgen Lake shows that they ruptured at 3 ka (Nash, 1984).

Trenching and geomorphic analysis of the Hebgen Lake and Red Canyon Faults determined slip rates of 0.1–0.5 mm/yr (0.004–0.02 in/yr; e.g., Kogan and Bendick, 2011; Ruleman and others, 2014). GNSS data indicate that modern extension across the Hebgen Lake Fault may be as high as 3.0–3.6 mm/yr (0.12–0.14 in/yr; Puskas and others, 2007). However, GNSS results may not accurately represent long-term extension rates, because viscoelastic deformation of the lower crust in response to the 1959 earthquake may alter measured station velocities by as much as 1 mm/yr (0.04 in/yr; Nishimura, 2003; Puskas and others, 2007).

Extension in the Hebgen basin and the area surrounding the Hebgen Lake and Red Canyon Faults may be faster than that estimated across individual faults. Baseline length measurements carried out after the 1959 earthquake estimated the positions of individual sites in the Hebgen basin between 1973 and 1987 (Savage and others, 1993). Changes in distances between sites over time indicate that extension in the Hebgen basin is as high as 8 mm/yr (0.3 in/yr). These high extension rates may reflect magma intrusions associated with the Yellowstone caldera (Savage and others, 1993). This interpretation is consistent with InSAR and GNSS data, which imply lateral displacement of 70 mm/yr in the east–west direction, and 20 mm/yr in the north–south direction related to magma migration (Aly and Cochran, 2011).

The Madison Fault

The north-striking, west-dipping Madison Fault is located northwest of the Hebgen basin (fig. 1). A 2.4 km (1.5 mi) section of the Madison Fault ruptured during the 1959 Hebgen Lake earthquake, and produced a series of discontinuous ~1 m (3 ft) high "scarplets" (Mathieson, 1983; Myers and Hamilton, 1964). Debate remains as to whether the 1959 Madison Fault scarps represented sympathetic slip resulting from down-to-the-south slip on an underlying east–west fault (Myers and Hamilton, 1964) or primary rupture on a valley-bounding fault (Witkind, 1964). Geomorphic analysis of scarps unaffected by the 1959 earthquake shows that the Madison Fault previously ruptured at 1–5 ka (Ruleman and Lageson, 2002). Fault scarps locally offset Pinedale (30–10 ka) glacial deposits by 1–12 m (3–40 ft; Lundstrom, 1986; Mathieson, 1983; Ruleman and Lageson, 2002), with offsets of >2 m (>7 ft) likely produced by multiple rupture events (Mathieson, 1983). The variable offset of Pinedale glacial deposits along the length of the fault then implies that the Madison Fault ruptures in individual segments, with each rupture producing cumulative offset on one or more segments. Seismicity and geologic mapping confirm the existence of five separate fault segments with distinct rupture histories (Ruleman and Lageson, 2002).

The Madison Valley also contains a number of prominent fluvial risers, which are likely associated with glacial and periglacial processes (Schneider, 1994). Fluvial risers occur between fluvial terraces along the Madison River (fig. 4; Schneider, 1994). Fluvial terraces in the Madison Valley likely record

deposition from upstream glacial outburst floods during both the Bull Lake and Pinedale glaciations (Lundstrom, 1986). The Madison River subsequently incised these deposits up to 60 m (197 ft), creating prominent paired terraces on both sides of the river (Lundstrom, 1986).

A discrepancy between long-term (Myr) and short-term (kyr) slip rates, combined with geomorphic analysis of degraded fault scarps, indicate that the Madison Fault may experience earthquake clustering, with some periods of geologic time having greater seismic activity than others (Mathieson, 1983; Ruleman and Lageson, 2002). The Madison Fault offsets the 2.1 Ma Huckleberry Ridge Tuff by ~1,000 m (~3,280 ft), yielding a long-term slip rate of ~0.5 mm/yr (0.02 in/yr). Offset deposits associated with the (200–135 ka) Bull Lake glaciation and the (30–10 ka) Pinedale glaciation provide short-term slip rate estimates. Fault-scarp profiles and geologic mapping indicate that the Madison Fault had a much lower slip rate of 0.01–0.04 mm/yr (0.0004–0.0016 in/yr) since the Bull Lake glaciation and prior to the Pinedale glaciation (approx. 135–30 ka; Mathieson, 1983). Analysis of offset deposits associated with the Pinedale glaciation shows that slip rates since ~15 ka may be closer to long-term averages, at 0.3–0.4 mm/yr (0.012–0.016 in/yr; Mathieson, 1983).

Maximum credible earthquake magnitudes and estimates of earthquake recurrence intervals are variable for the Madison Fault because they are based on observed single event fault offsets. Quaternary surface offsets support both 1 m (3.3 ft) and 3 m (10 ft) single event offsets, which correspond with M 6.8 and M 7.3 earthquakes based on empirical correlations by Slemmons (1977). A comparison between these single event values and total offsets on Quaternary surfaces then suggests that M 6.8 and M 7.3 earthquakes would respectively have recurrence intervals of 1.9–3.8 ka and 7.5–10 ka (Mathieson, 1983). More recent geomorphic analysis of fault scarps along the Madison Fault instead indicates a maximum credible earthquake of M 6.5 to M 7.1 with a recurrence interval of <10 ka (Ruleman and Lageson, 2002).

The Lima Reservoir Fault

The Lima Reservoir Fault is located west of Hebgen Lake and is also affected by the Yellowstone hotspot (fig. 1). This east-striking, south-dipping normal fault lies on the north side of the Centennial Valley, in an area of elevated topography that was likely affected by the Yellowstone hotspot (Anastasio and others, 2010; Anders and others, 1989; fig. 1). The Lima Reservoir Fault consists of three primary sections: (1) the Henry Gulch, (2) the Reservoir, and (3) the Trail Creek. These segments have an overall slip rate of 0.31 mm/yr (0.012 in/yr; Anastasio and others, 2010).

Paleoseismic investigations of the Lima Reservoir Fault describe the rupture histories of each fault segment and suggest its relationship to regional tectonic processes. Trenching along the Lima Reservoir Fault reveals eight seismic events since 45 ka. Fault slip vectors determined during trenching show that this fault has two primary modes of fault slip: (1) normal, to accommodate north–south extension associated with the Yellowstone hotspot; and (2) oblique, to accommodate northeast–southwest extension associated with normal faulting in the Basin and Range Province. Recurrence intervals for normal faulting are estimated at 10–15 ka, with a 1–3 ka recurrence interval for oblique-slip events (Bartholomew and others, 2009a). Fault scarp diffusion modeling, combined with ^{14}C and optically stimulated luminescence (OSL) dating of offset surfaces, indicates that the Lima Reservoir Fault experienced seismic events at >50 ka, 23 ka, 13 ka, and 8 ka. The 8 ka and 23 ka or 10 ka events likely affected multiple fault segments. Seismic clustering and coincident events on multiple fault segments imply connectivity between fault segments. Modern streams have not been offset by the Lima Reservoir Fault, indicating that the 8 ka age represents the most recent seismic event (Anastasio and others, 2010).

The Centennial Fault

The Centennial Fault marks the northern boundary of high topography immediately north of the Snake River Plain. This west-striking and north-dipping fault lies to the south of the Lima Reservoir Fault across the Centennial Valley (fig. 1). The Centennial Fault offsets the 2.1 Ma Huckleberry Ridge Tuff, implying that this unit represents a minimum age for the initiation of the Centennial Fault. Fault scarp profiles along the length of the fault show that glacial deposits are offset by an average of 9.1–9.6 m (30–32 ft). If these glacial deposits are associated with the Pinedale glaciation (at about 12 ka), the slip rate of the Centennial Fault is likely 0.65 to 0.82 mm/yr (0.026–0.032 in/yr). If offset glacial sediments are older, for example associated with the (200–135 ka) Bull Lake glaciation, slip rates on the fault would be <0.1 mm/yr (<0.004 in/

yr; Petrik, 2008). Wong and others (2005) proposed a slip rate of 1.3 mm/yr (0.05 in/yr) for the Centennial Fault, based on a weighted mean of slip rates derived from geodetic data, offset Quaternary strata, the offset Huckleberry Ridge Tuff, and gravity data.

The Red Rock and Monument Hill Faults

The Red Rock Valley is located west of the Centennial Valley and is bounded by the northwest-striking Red Rock and Monument Hill Faults (fig. 1). The Red Rock Fault lies at the southwest end of the valley and dips to the east. The Monument Hill Fault lies at the northeast end of the valley and dips to the west (e.g., Harkins and others, 2005). The most recent event on the Red Rock Fault likely occurred at ~3.7 ka, based on ^{14}C dates of an offset soil. A horizon in a trench across the fault (Bartholomew and others, 2009b). Harkins and others (2005) used soil profile analyses, coupled with ^{14}C ages, to estimate the ages of offset surfaces along the Red Rock Fault, and combined the results with alluvial fan and stream morphologies to estimate along-strike changes in slip rates. Their results show that the fault may be delineated into three primary segments (e.g., Crider and Pollard, 1998), with distinct but overlapping rupture histories. Estimated fault slip rates are highest in the south, closest to the Centennial Fault and the Yellowstone hotspot, decreasing to the north. The southernmost segment has maximum slip rates of 1.3–2.0 mm/yr (0.05–0.08 in/yr), the central segment has an estimated maximum slip rate of 0.6–0.9 mm/yr (0.02–0.04 in/yr), whereas the northern segment has minimal offset and likely has not ruptured since late Pleistocene time.

Regalla and others (2007) investigated the rupture history of the Monument Hill Fault system using fault scarp profile analysis, geomorphic mapping, and ages of offset surfaces based on soil profile investigations coupled with ^{14}C dates. Geologic mapping of the Monument Hill Fault shows fault scarps along three parallel and synthetic fault segments. Analysis of all three fault segments implies that the Monument Hill Fault has experienced earthquake clustering at 22–32 ka and >160 ka. However, the most recent event along this fault has not been identified, owing to the lack of observable fault scarps in the youngest deposits. Regalla and others (2007) concluded that the distinct rupture histories of the Monument Hill and Red Rock Faults imply that they are not linked at depth. Instead, they proposed that the two faults are connected by an accommodation zone, which accommodates extension through broad folding and oblique slip on smaller faults at depth. This accommodation zone may be controlled by an older compressional transfer zone associated with the Sevier Fold-Thrust Belt.

The Blacktail Fault

The Beaverhead River Canyon lies to the north of the Red Rock Valley, and trends to the northeast. The Beaverhead River emerges from the Beaverhead River Canyon, where it intersects the western end of the northwest-striking Blacktail Fault that bounds the northeast flank of the Blacktail Mountains (fig. 1). The Beaverhead River Canyon contains paired terraces at approximately 11, 34, 65, and 75 m (36, 112, 213, and 246 ft) above the modern river. A terrace lying at 39 m (128 ft) above the Beaverhead River contains a tufa that was dated at 90 ka using U-Th disequilibrium series dating, yielding a 0.43 mm/yr (0.02 in/yr) incision rate (Bartholomew and others, 1999). This incision rate yields a ~180 ka age for the oldest terraces, and a ~460 ka age for the initiation of incision into the Beaverhead River Canyon (Bartholomew and others, 1999).

The Blacktail Fault contains a subtle fault scarp that extends to within 11 km (6.8 mi) of the Beaverhead River Canyon. However, field investigations provide no clear evidence for Holocene offset along the Blacktail Fault (Bartholomew and others, 1999). Farther to the southeast, 29 km (18 mi) from the Beaverhead River Canyon, older glacial sediments are offset in a paleoseismic trench. These glacial sediments are inferred to be of Bull Lake age (120 ka) and are offset by 6.5 m (21 ft), yielding a fault slip rate of ~0.05 mm/yr (~0.002 in/yr) (Bartholomew and others, 1999). Thick Holocene colluvium and well-developed soils found on the downthrown side of the fault during trenching imply that the last rupture occurred between the Bull Lake and Pinedale glaciations. Because incision of the Beaverhead River is an order of magnitude faster than slip on the Blacktail Fault, faulting likely plays a minimal role in driving fluvial incision and terrace formation through base level lowering on the downthrown side of the fault (Bartholomew and others, 1999).

Townsend and Clarkston Valleys

The Clarkston Valley is a narrow northeast-trending valley located west of the Big Belt Mountains (fig. 1). The Clarkston Valley is located at the eastern edge of the Lewis and Clark zone, a broad

area of transtension that cuts across western Montana (Foster and others, 2007; fig. 1). The Clarkston Valley contains the Missouri River and the Toston Dam, which was a site of a previous seismic assessment (Wong and others, 1999). Wong and others (1999) compiled regional geologic data and field surveys, and identified six major Quaternary faults: the Clarkston Valley, Beaver Creek, Bridger, Upper Sixmile Creek, Canyon Ferry, and Toston Faults. The Beaver Creek Fault is located north of the Clarkston Valley on the southwestern edge of the Townsend Valley, is northwest to northerly striking, and dips to the east. Remaining faults are northeast- to northwest-striking, and dip to the west. The Clarkston Valley Fault is located on the eastern edge of the Clarkston Valley. The Bridger Fault lies at the western edge of the Bridger Range. Remaining faults lie on the eastern edge of the Townsend Valley, with the Toston Fault possibly being a distinct southerly fault segment of the Canyon Ferry Fault. Scarps on the Toston Fault are ~8 m (~26 ft) high, and up to 31 m (102 ft) high on the Upper Sixmile Creek Fault. The Upper Sixmile Creek Fault is a bedrock fault covered by a mantle of Quaternary deposits and colluvium, implying that it has not been active since early Quaternary time. The Bridger Fault contains no notable fault scarps in its southern half, though it may offset alluvial deposits of uncertain age at its northern end. Total offset on the Bridger Fault may be up to 2.2 km (1.4 mi), but the history of the fault and age of last rupture remain uncertain. The age of the Beaver Creek Fault is currently unknown, but may be older than 750 ka based on scarp morphologies. The Toston Fault offsets Quaternary alluvium, and may have been the site of the 1925 Clarkston Valley earthquake, indicating that it may have been active in Quaternary time. Wong and others (1999) report that the Clarkston Valley Fault may offset Quaternary deposits. The Clarkston Valley Fault is the most likely site of the 1925 Clarkston Valley earthquake, though no fault scarps associated with this event have been located (Pardee, 1926; Wong and others, 1999). More recent mapping does not show the Clarkston Valley Fault as offsetting Quaternary deposits, indicating that it may not have been active in Quaternary time (Vuke and Stickney, 2013). Estimates of maximum credible earthquake magnitudes on these faults vary between $\mathbf{M}_w$ 6.75 and 7.25 (Wong and others, 1999).

The Canyon Ferry Fault is located at the northeast end of the Townsend Valley, at the western edge of the Big Belt Mountains (fig. 1). The Canyon Ferry Fault lies at the eastern end of the Lewis and Clark Line. It has a northerly strike through most of the Townsend Valley, and curves to a westerly strike at the northern edge of the valley (Andersen and LaForge, 2003). A fault trench and associated infrared stimulated luminescence dates, as well as fault scarp profiles, indicate that the Canyon Ferry Fault has not ruptured since 13 ka (Andersen and LaForge, 2003). As with other faults in Montana, trenching and age dates indicate periods of earthquake clustering, in this case between 21 and 13 ka. Long-term slip rates on the Canyon Ferry Fault are estimated at 0.16 mm/yr (0.006 in/yr), though trenching indicates short-term slip rates may be as high as 0.54 mm/yr (0.02 in/yr) during earthquake clusters (Andersen and LaForge, 2003). A total of 9 m (30 ft) of slip between 68 and 13 ka is estimated from the trench log (Andersen and LaForge, 2003). Faulting west of the Canyon Ferry Fault in the Helena Valley offsets Pleistocene surfaces, showing that faults in this area have been active prior to the 1935 Helena earthquake (Stickney, 1987).

The Flathead and Mission Valleys

The Mission Fault of northwestern Montana lies at the eastern edge of the Mission Valley and at the western edge of the Mission Mountains (fig. 1). It is a south-striking, west-dipping normal fault composed of a single strand south of Flathead Lake, but breaks into multiple fault segments in the Flathead Valley to the north (Hofmann and others, 2006). The Mission Fault marks either the northernmost extent of the Basin and Range Province or the southernmost segment of the Rocky Mountain Trench (Hofmann and others, 2006; Lageson and Stickney, 2000). The Mission Fault offsets glacial deposits in the Mission Valley, and synthetic faults have deformed Quaternary lake sediments in Flathead Lake (Hofmann and others, 2006; Ostenaa and others, 1995). Trenching investigations along the Mission Fault indicate that the most recent seismic event occurred at 7.7 ± 0.2 ka. ^{14}C and OSL ages of offset deposits, as well as the ~6.8 ka Mazama ash present in six trenches, provide a record of seismic events up to ~30 ka (Ostenaa and others, 1995). This record yields a recurrence interval of major earthquakes along the Mission Fault at 4–8 kyr. The length of the Mission Fault yields a maximum credible earthquake of $\mathbf{M}_s$ 7.5 based on comparison with the $\mathbf{M}_s$ 7.5 1959 Hebgen Lake, $\mathbf{M}_s$ 7.3 1983 Borah Peak, and $\mathbf{M}_s$ 7.1 Fairview Peak earthquakes, which ruptured faults of a similar length (Ostenaa and others, 1995).

Deformation in the Flathead Valley evolves from the single-strand Mission Fault across Mission Valley to a system of normal faults forming a broad graben in Flathead Lake. Seismic investigations of Flathead Lake, coupled with lake sediment cores, geologic mapping, and ^{14}C ages, provide additional constraints on the history of faulting in Flathead Lake. Records of deformation go back to 15 ka, with the youngest event dated at 1.5 ka (Hofmann and others, 2006). Deformation typically occurs in clusters with a higher frequency of deformation events occurring at specific time intervals. These clustering events have a recurrence interval of ~3 ka and appear to be coeval across multiple faults and fault segments (Hofmann and others, 2006). Displacement rates of the lake basin, including multiple faults, range between 0.08 and 1 mm/yr (0.003 and 0.04 in/yr). Slip rates on individual faults are typically lower, from 0.03 to 0.43 mm/yr (0.001 to 0.017 in/yr; Hofmann and others, 2006).

Landslides as Paleoseismic Records

Landslide deposits record periods of high rainfall, deglaciation, and/or seismicity (e.g., Buller and others, 1998; Carrara and O'Neill, 2003; Smith, 2001). In large parts of Montana, vegetation obscures old landslides. New high-resolution topographic data using LiDARelevation data has revealed that parts of Montana contain pervasive and heretofore unknown landslides (Vuke, 2013). As LiDAR data become more widely available, additional investigations will likely increase the number of old landslides on geologic maps, with direct or relative age dating providing a sense of landslide periodicity. Combined, these data will help with future assessments of regional landslide and seismic hazards.

Trees located on or above landslides and fault scarps may record periods of local or regional seismicity (Bekker, 2004; Carrara and O'Neill, 2003). Trees typically respond to landslide movement via a reduction in annual ring width, or the formation of reaction wood (Carrara and O'Neill, 2003). A study of three landslides in the Gravelly Range of southwestern Montana by Carrara and O'Neill (2003) proposes that tree ring records preserve landslide movement associated with major earthquakes in and near southwestern Montana dating back to 1908. Curiously, these tree ring data record the 1925 Clarkston Valley, 1935 Helena, and 1959 Hebgen Lake earthquakes, but not a nearby 1947 **M** 6.25 earthquake. Recorded seismic events were located up to 200 km away, showing that slow moving landslides may react to distant earthquakes (Carrara and O'Neill, 2003). These tree ring records indicate that landslide movements have a 22–26 year recurrence interval. This period of landslide movement may reflect regional background seismicity for the last century and provide a minimum limit for regional seismic hazard assessments (O'Neill and others, 1994). Alternatively, the 22–26 year period may represent a cycle of other landslide-triggering mechanisms, such as intense rainfall or snowmelt events that have yet to be identified. Additional dendrochronological investigations of slow-moving landslides in Montana would help bolster records of background seismicity, identify periodicity in landslide triggering, and improve regional hazard assessments.

SUMMARY AND FUTURE WORK

The neotectonic development of western Montana is a consequence of far-field stresses related to the interaction of the North American and Pacific plates combined with local stresses produced by the Yellowstone hotspot. These tectonic stresses are accommodated in modern time by normal, strike-slip, and transtensional oblique-slip faulting. Fault slip rates and earthquake recurrence intervals are unknown for most active faults in Montana. However, available data suggest that ground motion and surface rupture are a significant hazard for lives and infrastructure in western Montana. Additional paleoseismic studies of Quaternary faults would greatly improve regional seismic hazard assessments. Paleoseismic data could then be combined with geodetic investigations and thermochronometry to investigate the tectonic development of western Montana in Cenozoic time. Low-relief surfaces throughout Montana may have formed as a consequence of changes in the locus and style of extensional faulting, far-field base level changes, changes in climate, and/or dynamic topography. Future studies should investigate the formation mechanisms of low-relief surfaces using modern geochronology and geomorphology techniques and attempt to create a systematic framework to categorize such surfaces throughout the region.

ACKNOWLEDGMENTS

We are grateful to Zach Lifton and Steve Bowman, whose thorough and insightful comments helped improve the quality of the manuscript. Editorial support by John Metesh, Susan Vuke, Colleen Elliott, and Susan Barth helped make this manuscript possible.

REFERENCES

Alden, W.C., 1932, Physiography and glacial geology of eastern Montana and adjacent areas: U.S. Geological Survey Professional Paper 174, 133 p., doi: https://doi.org/10.3133/pp174

Alden, W.C., 1953, Physiography and glacial geology of western Montana and adjacent areas: U.S. Geological Survey Professional Paper 231, 200 p., doi: https://doi.org/10.3133/pp231

Aly, M.H., and Cochran, E.S., 2011, Spatio-temporal evolution of Yellowstone deformation between 1992 and 2009 from InSAR and GPS observations: Bulletin of Volcanology, v. 73, no. 9, p. 1407–1419, doi: https://doi.org/10.1007/s00445-011-0483-y

Anastasio, D.J., Majerowicz, C.N., Pazzaglia, F.J., and Regalla, C.A., 2010, Late Pleistocene– Holocene ruptures of the Lima Reservoir fault, SW Montana: Journal of Structural Geology, v. 32, no. 12, p. 1996–2008, doi: https://doi.org/10.1016/j.jsg.2010.08.012

Anders, M.H., Geissman, J.W., Piety, L.A, and Sullivan, J.T., 1989, Parabolic distribution of circumeastern Snake River Plain seismicity and latest Quaternary faulting: Migratory pattern and association with the Yellowstone hotspot: Journal of Geophysical Research, v. 94, no. B2, p. 1589–1621.

Andersen, L.W., and LaForge, R., 2003, Seismotectonic study for Canyon Ferry Dam, Missouri River Basin Project, Montana: Bureau of Reclamation Seismotectonic Reports, v. 2003-1.

Atwood, W.W., 1916, The physiographic conditions at Butte, Montana, and Bingham Canyon, Utah, when the copper ores in these districts were enriched: Economic Geology, v. 11, no. 8, p. 697–740.

Bartholomew, M.J., Bone, M.J., Rittenour, T.M., Mickelson, A.M., and Stickney, M.C., 2009a, "Stress switching" along the Lima Reservoir fault in Yellowstone's wake: Geological Society of America Abstracts with Programs, v. 41, no. 7, p. 55.

Bartholomew, M.J., Greenwell, R.A., and Stickney, M.C., 2009b, Alluvial fans: Sensitive tectonic indicators of fault-segmentation and stress-field partitioning along the Red Rock fault, southwestern Montana, USA: Northwest Geology, v. 38, p. 41–65.

Bartholomew, M.J., Lewis, S.E., Russell, G.S., Stickney, M.C., Wilde, E.M., and Kish, S.A., 1999, Late Quaternary history of the Beaverhead River Canyon, southwestern Montana, *in* Hughes, S.S., and Thackary, G.D. eds., Guidebook to the geology of eastern Idaho: Idaho Museum of Natural History, p. 237–250.

Becker, T.W., Faccenna, C., Humphreys, E.D., Lowry, A.R., and Miller, M.S., 2014, Static and dynamic support of western United States topography: Earth and Planetary Science Letters, v. 402, no. C, p. 234–246, doi: https://doi.org/10.1016/j.epsl.2013.10.012

Bekker, M.F., 2004, Spatial variation in the response of tree rings to normal faulting during the Hebgen Lake earthquake, southwestern Montana, USA: Dendrochronologia, v. 22, no. 1, p. 53–59, doi: https://doi.org/10.1016/j.dendro.2004.09.001

Bevan, A., 1923, Summary of the geology of the Beartooth Mountains, Montana: Journal of Geology, v. 31, no. 6, p. 441–465.

Bevan, A., 1925, Rocky Mountain peneplains northeast of Yellowstone Park: Journal of Geology, v. 33, no. 6, p. 563–587.

Brocher, T.M., Wells, R.E., Lamb, A.P., and Weaver, C.S., 2017, Evidence for distributed clockwise rotation of the crust in the northwestern United States from fault geometries and focal mechanisms: Tectonics, v. 36, no. 5, p. 787–818, doi: https://doi.org/10.1002/2016TC004223

Buller, D.R., Malanson, G.P., Wilkerson, F.D., and Schmid, G.L., 1998, Late Holocene sturzstroms in Glacier National Park, Montana, USA, *in* Geomorphological hazards in high mountain areas: Dordrecht, The Netherlands, Springer, p. 149–166.

Carrara, P.E., and O'Neill, J.M., 2003, Tree-ring dated landslide movements and their relationship to seismic events in southwestern Montana, USA: Quaternary Research, v. 59, no. 1, p. 25–35, doi: https://doi.org/10.1016/S0033-5894(02)00010-8

Crider, J.G., and Pollard, D.D., 1998, Fault linkage: Three-dimensional mechanical interaction between echelon normal faults: Journal of Geophysical Research: Solid Earth, v. 103, no. B10, p. 373–391, doi: https://doi.org/10.1029/98JB01353

Crone, A.J., and Haller, K.M., 1991, Segmentation and the coseismic behavior of Basin and Range normal faults: Examples from east-central Idaho and southwestern Montana, U.S.A.: Journal of Structural Geology, v. 13, no. 2, p. 151–164, doi: https://doi.org/10.1016/0191-8141(91)90063-O

Deng, J., 1998, Viscoelastic flow in the lower crust after the 1992 Landers, California, earthquake: Science, v. 282, no. 5394, p. 1689–1692, doi: https://doi.org/10.1126/science.282.5394.1689

Dickinson, W.R., 2006, Geotectonic evolution of the Great Basin: Geosphere, v. 2, no. 7, p. 353–368, doi: https://doi.org/10.1130/GES00054.1

Doser, D.I., 1985, Source parameters and faulting processes of the 1959 Hebgen Lake, Montana, earthquake sequence: Journal of Geophysical Research: Solid Earth, v. 90, no. B6, p. 4537–4555.

Dresser, H., 1996, Hugh Dresser pictorial guides: A stereo picture to some faults, fans, and pediments of southwestern Montana: Montana Bureau of Mines and Geology Open-File Report 656-J, 57 p.

Ekström, G., Nettles, M., and Dziewoński, A.M., 2012, The global CMT project 2004–2010: Centroid-moment tensors for 13,017 earthquakes: Physics of the Earth and Planetary Interiors, v. 200–201, p. 1–9, doi: https://doi.org/10.1016/j.pepi.2012.04.002

Farr, T.G., Rosen, P.A., Caro, E., Crippen, R., Duren, R., Hensley, S., Kobrick, M., Paller, M., Rodriguez, E., Roth, L. and Seal, D., 2007, The shuttle radar topography mission: Reviews of Geophysics, v. 45, no. 2, p. 1–33, doi: https://doi.org/10.1029/2005RG000183

Fields, R.W., Rasmussen, D.L., Tabrum, A.R., and Nichols, R., 1985, Cenozoic rocks of the intermountain basins of western Montana and eastern Idaho: A summary, in Flores, R.M., and Kaplan, S.S., eds., Cenozoic Paleogeography of West-Central United States: Rocky Mountain Section, Society of Economic and Petroleum Geologists, p. 9–36.

Foster, D.A., Doughty, P.T., Kalakay, T.J., Fanning, C.M., Coyner, S., Grice, W.C., and Vogl, J., 2007, Kinematics and timing of exhumation of metamorphic core complexes along the Lewis and Clark fault zone, northern Rocky Mountains: Geological Society of America Special Paper, v. 434, no. 10, p. 207–232, doi: https://doi.org/10.1130/2007.2434(10)

Fuentes, F., DeCelles, P.G., Constenius, K.N., and Gehrels, G.E., 2011, Evolution of the Cordilleran Foreland Basin System in northwestern Montana, U.S.A.: Geological Society of America Bulletin, v. 123, no. 3–4, p. 507–533, doi: https://doi.org/10.1130/GES00773.1

Guerrero, E.F., 2017, Quaternary landscape evolution and the surface expression of plume-lithosphere interactions in the greater Yellowstone area: Corvallis, Oregon State University, Ph.D. dissertation, 125 p.

Hadley, J.B., 1964, Landslides and related phenomena accompanying the Hebgen Lake earthquake of August 17, 1959: U.S. Geological Survey Professional Paper 435–K, p. 107–138, doi: https://doi.org/10.3133/pp435

Hadley, R.F., 1967, Pediments and pediment-forming processes: Journal of Geological Education, v. 15, no. 2, p. 83–89.

Haller, K.M., Tsutsumi, H., Machette, M.N., Essex, J., and Hancock, D., 2002, Paleoseismic investigation of the 1959 Red Canyon fault, southwestern Montana: Geological Society of America Abstracts with Programs, v. 34, p. A-4.

Hanneman, D.L., Cheney, E.S., and Wideman, C.J., 2003, Cenozoic sequence stratigraphy of northwestern USA: Cenozoic Systems of the Rocky Mountain region, p. 135–155.

Harkins, N.W., Anastasio, D.J., and Pazzaglia, F.J., 2005, Tectonic geomorphology of the Red Rock fault, insights into segmentation and landscape evolution of a developing range front normal fault: Journal of Structural Geology, v. 27, no. 11, p. 1925–1939, doi: https://doi.org/10.1016/j.jsg.2005.07.005

Herrmann, R.B., Benz, H., and Ammon, C.J., 2011, Monitoring the earthquake source process in North America: Bulletin of the Seismological Society of America, v. 101, no. 6, p. 2609–2625, doi: https://doi.org/10.1785/0120110095

Hofmann, M.H., Hendrix, M.S., Sperazza, M., and Moore, J.N., 2006, Neotectonic evolution and fault geometry change along a major extensional fault system in the Mission and Flathead Valleys, NW-Montana: Journal of Structural Geol-

ogy, v. 28, no. 7, p. 1244–1260, doi: https://doi.org/10.1016/j.jsg.2006.03.030

Janecke, S.U., and Blankenau, J.J., 2003, Extensional folds associated with Paleogene detachment faults in SE part of the Salmon basin: Northwest Geology, p. 51–73.

Kobayashi, D., Sprenke, K.F., Stickney, M.C., and Phillips, W.M., 2016, Seismotectonic interpretation of the 2015 Sandpoint, Idaho, earthquake sequence: Idaho Geological Survey, Staff Report 16–1.

Kogan, L., and Bendick, R., 2011, A mass failure model for the initial degradation of fault scarps, with application to the 1959 scarps at Hebgen Lake, Montana: Bulletin of the Seismological Society of America, v. 101, no. 1, p. 68–78, doi: https://doi.org/10.1785/0120100107

Kuenzi, W.D., and Fields, R.W., 1971, Tertiary stratigraphy, structure and geologic history, Jefferson Basin, Montana: Geological Society of America Bulletin, v. 82, p. 3374–3394.

Lageson, D.R., and Stickney, M.C., 2000, Seismotectonics of northwest Montana, USA, *in* Schalla, R.A., and Johnson, E.H., eds., Montana/Alberta thrust belt and adjacent foreland: Montana Geological Society 50th Anniversary Symposium, v. 1, p. 109–126.

Lindsey, D.A., 1982, Geologic map and discussion of selected mineral resources of the North and South Moccasin Mountains, Fergus County, Montana: U.S. Geological Survey Miscellaneous Investigations I-1362, scale 1:24,000, doi: https://doi.org/10.3133/i1362

Lowry, A.R., and Pérez-Gussinyé, M., 2011, The role of crustal quartz in controlling Cordilleran deformation: Nature, v. 471, no. 7338, p. 353–359, doi: https://doi.org/10.1038/nature09912

Lowry, A.R., Ribe, N.M., and Smith, R.B., 2000, Dynamic elevation of the Cordillera, western United States: Journal of Geophysical Research, v. 105, no. B10, p. 23371–23390, doi: https://doi.org/10.1029/2000JB900182

Lundstrom, S.C., 1986, Soil stratigraphy and scarp morphology studies applied to the Quaternary geology of the southern Madison Valley, Montana: Arcata, California, Humboldt State University, M.S. thesis, 53 p.

Mathieson, E.L., 1983, Late Quaternary activity of the Madison fault along its 1959 rupture trace, Madison County, Montana: Stanford, California, Stanford University, M.S. thesis, 169 p.

McCaffrey, R., King, R.W., Payne, S.J., and Lancaster, M., 2013, Active tectonics of northwestern U.S. inferred from GPS-derived surface velocities: Journal of Geophysical Research: Solid Earth, v. 118, no. 2, p. 709–723, doi: https://doi.org/10.1029/2012JB009473

McCaffrey, R., Qamar, A.I., King, R.W., Wells, R., Khazaradze, G., Williams, C.A., Stevens, C.W., Vollick, J.J., and Zwick, P.C., 2007, Fault locking, block rotation and crustal deformation in the Pacific Northwest: Geophysical Journal International, v. 169, no. 3, p. 1315–1340, doi: https://doi.org/10.1111/j.1365-246X.2007.03371.x

McQuarrie, N., and Rodgers, D.W., 1998, Subsidence of a volcanic basin by flexure and lower crustal flow: The eastern Snake River Plain, Idaho: Tectonics, v. 17, no. 2, p. 203–220, doi: https://doi.org/10.1029/97TC03762

Montagne, J., and Chadwick, R.A., 1982, Cenozoic history of the Yellowstone Valley south of Livingston, Montana: Rocky Mountain Section of the Geological Society of America Thirty-Fifth Annual Field Conference, 67 p.

Myers, W.B., and Hamilton, W., 1964, Deformation accompanying the Hebgen Lake earthquake of August 17th, 1959: U.S. Geological Survey Professional Paper 435, p. 55–98, doi: https://doi.org/10.3133/pp435

Nash, D.B., 1984, Morphologic dating of fluvial terrace scarps and fault scarps near West Yellowstone, Montana: Geological Society of America Bulletin, v. 95, no. 12, p. 1413, doi: https://doi.org/10.1130/0016-7606(1984)95%3C1413:MDOFTS%3E2.0.CO;2

Nemkin, S.R., Lageson, D.R., van der Pluijm, B., and Van der Voo, R., 2016, Remagnetization and folding in the frontal Montana Rocky Mountains: Lithosphere, v. 8, no. 6, p. 716–728, doi: https://doi.org/10.1130/L579.1

Nishimura, T., 2003, Rheology of the lithosphere inferred from postseismic uplift following the 1959 Hebgen Lake earthquake: Journal of Geophysical Research: Solid Earth, v. 108, no. B8, 12 p., doi: https://doi.org/10.1029/2002JB002191

O'Neill, J.M., LeRoy, T.H., and Carrara, P.E., 1994, Preliminary map showing Quaternary faults and landslides in the Cliff Lake 15' quadrangle, Madison County, Montana: U.S. Geological Survey Open-File Report 94-198, scale 1:62,500.

Olson, N.H., Dilles, J.H., Kallio, I.M., Horton, T.R., and Scarberry, K.C., 2016, Geologic map of the Ratio Mountain 7.5' quadrangle, southwest Montana: Montana Bureau of Mines and Geology EDMAP 10, scale 1:24,000.

Ostenaa, D.A., Levish, D.R., and Klinger, R.E., 1995, Mission fault study: U.S. Bureau of Reclamation Seismotectonic Report no. 94-8.

Pardee, J.T., 1926, The Montana earthquake of June 28, 1925: U.S. Geological Survey Professional Paper 147-B, p. 7–23.

Pardee, J.T., 1950, Late Cenozoic block faulting in western Montana: Geological Society of America Bulletin, v. 61, no. 4, p. 359, doi: https://doi.org/10.1130/0016-7606(1950)61[359:LCBFIW]2.0.CO;2

Parker, S.D., 2016, Tectonic alteration of a major Neogene river drainage of the Basin and Range: Missoula, University of Montana, M.S. thesis, 115 p.

Payne, S.J., McCaffrey, R., and Kattenhorn, S.A., 2013, Extension-driven right-lateral shear in the Centennial shear zone adjacent to the eastern Snake River Plain, Idaho: Lithosphere, v. 5, no. 4, p. 407–419, doi: https://doi.org/10.1130/L200.1

Payne, S.J., McCaffrey, R., and King, R.W., 2008, Strain rates and contemporary deformation in the Snake River Plain and surrounding Basin and Range from GPS and seismicity: Geology, v. 36, no. 8, p. 647–650, doi: https://doi.org/10.1130/G25039A.1

Peng, X., and Humphreys, E.D., 1998, Crustal velocity structure across the eastern Snake River Plain and the Yellowstone swell: Journal of Geophysical Research: Solid Earth, v. 103, no. B4, p. 7171–7186, doi: https://doi.org/10.1029/97JB03615

Petersen, M.D., Moschetti, M.P., Powers, P.M., Mueller, C.S., Haller, K.M., Frankel, A.D., Zeng, Y., Rezaeian, S., Harmsen, S.C., Boyd, O.S., Field, E.H., Chen, R., Luco, N., Wheeler, R.L., and others, 2014, Seismic-hazard maps for the conterminous United States: U.S. Geological Survey Scientific Investigations Map SI-3325, scale 1:7,000,000.

Petrik, F.E., 2008, Scarp analysis of the Centennial normal fault, Beaverhead County, Montana and Fremont County, Idaho: Bozeman, Montana State University, M.S. thesis, 207 p.

Pierce, K.L., and Morgan, L.A., 2009, Is the track of the Yellowstone hotspot driven by a deep mantle plume?—Review of volcanism, faulting, and uplift in light of new data: Journal of Volcanology and Geothermal Research, v. 188, no. 1–3, p. 1–25, doi: https://doi.org/10.1016/j.jvolgeores.2009.07.009

Pollitz, F.F., Bürgmann, R., and Banerjee, P., 2006, Post-seismic relaxation following the great 2004 Sumatra-Andaman earthquake on a compressible self-gravitating Earth: Geophysical Journal International, v. 167, no. 1, p. 397–420, doi: https://doi.org/10.1111/j.1365-246X.2006.03018.x

Puskas, C.M., and Smith, R.B., 2009, Intraplate deformation and microplate tectonics of the Yellowstone hot spot and surrounding western U.S. interior: Journal of Geophysical Research: Solid Earth, v. 114, no. 4, 23 p., doi: https://doi.org/10.1029/2008JB005940

Puskas, C.M., Smith, R.B., Meertens, C.M., and Chang, W.L., 2007, Crustal deformation of the Yellowstone–Snake River Plain volcano-tectonic system: Campaign and continuous GPS observations, 1987–2004: Journal of Geophysical Research: Solid Earth, v. 112, no. B3, p. 1–19, doi: https://doi.org/10.1029/2006JB004325

Regalla, C.A., Anastasio, D.J., and Pazzaglia, F.J., 2007, Characterization of the Monument Hill fault system and implications for the active tectonics of the Red Rock Valley, southwestern Montana: Journal of Structural Geology, v. 29, no. 8, p. 1339–1352, doi: https://doi.org/10.1016/j.jsg.2007.04.006

Reshkin, M., 1963, Geomorphic history of the Jefferson Basin, Jefferson, Madison, and Silver Bow Counties, Montana: Bloomington, Indiana University, Ph.D. dissertation, 146 p.

Reynolds, M.W., 1979, Character and extent of Basin-Range faulting, western Montana and east-central Idaho, *in* Newman, G., and Goode, H. eds., 1979 Basin and Range Symposium: Rocky

Mountain Association of Geologists and Utah Geological Association, p. 185–193.

Ritter, D.F., Kochel, R.C., and Miller, J.R., 2011, Process geomorphology: Long Grove, Ill., Waveland Press, Inc., 652 p.

Ruleman, C.A., and Lageson, D.R., 2002, Late Quaternary tectonic activity along the Madison fault zone, southwest Montana: Geological Society of America Abstracts with Programs, v. 33, no. 4, p. 12.

Ruleman, C., Larsen, M., and Stickney, M.C., 2014, Neotectonics and geomorphic evolution of the northwestern arm of the Yellowstone Tectonic Parabola: Controls on intra-cratonic extensional regimes, southwest Montana, in Shaw, C.A., and Tikoff, B., eds, Exploring the Northern Rocky Mountains: Geological Society of America Field Guide 37, no. 3, p. 65–87, doi: https://doi.org/10.1130/2014.0037(03)

Savage, J.C., Lisowski, M., Prescott, W.H., and Pitt, A., 1993, Deformation from 1973 to 1987 in the epicentral area of the 1959 Hebgen Lake, Montana, earthquake (**M**s=7.5): Journal of Geophysical Research: Solid Earth, v. 98, no. B2, p. 2145–2153, doi: https://doi.org/10.1029/92JB02410

Schmeelk, D., Bendick, R., Stickney, M.C., and Bomberger, C., 2017, Kinematic evidence for the effect of changing plate boundary conditions on the tectonics of the northern U.S. Rockies: Tectonics, v. 36, no. 6, p. 1–13, doi: https://doi.org/10.1002/2016TC004427

Schneider, N.P., 1994, Late Tertiary and Quaternary history of the Madison River Valley, southwest Montana: Carbondale, Southern Illinois University, Ph.D. dissertation, 330 p.

Schwartz, T.M., Methner, K., Chamberlain, C.P., Mulch, A., and Graham, S.A., 2019, Paleogene topographic and climatic evolution of the northern Rocky Mountains from integrated sedimentary and isotopic data: Geological Society of America Bulletin, v. 131, no. 7–8, p. 1203–1223.

Sears, J.W., Hendrix, M.S., Thomas, R.C., and Fritz, W.J., 2009, Stratigraphic record of the Yellowstone hotspot track, Neogene Sixmile Creek Formation grabens, southwest Montana: Journal of Volcanology and Geothermal Research, v. 188, no. 1–3, p. 250–259, doi: https://doi.org/10.1016/j.jvolgeores.2009.08.017

Shervais, J.W., Vetter, S.K., and Hanan, B.B., 2006, Layered mafic sill complex beneath the eastern Snake River Plain: Evidence from cyclic geochemical variations in basalt: Geology, v. 34, no. 5, p. 365–368, doi: https://doi.org/10.1130/G22226.1

Simons, F.S., and Armbrustmacher, T.J., 1976, High-level plateaus of the southeastern Beartooth Mountains, Montana and Wyoming—Remnants of an exhumed sub-Cambrian marine plain: Journal of Research of the U.S. Geologic Survey, v. 4, no. 4, p. 387–396.

Slemmons, D.B., 1977, Faults and earthquake magnitude: U.S. Army Corps of Engineers, Waterways Experimental Station, Miscellaneous Papers S-73-1, Report 6, p. 1–129.

Smith, L.N., 2001, Columbia Mountain landslide: Late-glacial emplacement and indications of future failure, northwestern Montana, USA: Geomorphology, v. 41, no. 4, p. 309–322, doi: https://doi.org/10.1016/S0169-555X(01)00062-9

Stickney, M.C., 1987, Quaternary geologic map of the Helena Valley, Montana: Montana Bureau of Mines and Geology, Geologic Map 46, scale 1:48,000.

Stickney, M.C., and Bartholomew, M.J., 1987, Seismicity and late Quaternary faulting of the northern Basin and Range Province, Montana and Idaho: Bulletin of the Seismological Society of America, v. 77, no. 5, p. 1602–1625.

Stickney, M.C., Haller, K.M., and Machette, M.N., 2000, Quaternary faults and seismicity in western Montana: Montana Bureau of Mines and Geology Special Publication 114, scale 1:750,000.

Styron, R.H., and Hetland, E.A., 2015, The weight of the mountains: Constraints on tectonic stress, friction, and fluid pressure in the 2008 Wenchuan earthquake from estimates of topographic loading: Journal of Geophysical Research: Solid Earth, v. 120, no. 4, p. 2697–2716, doi: https://doi.org/10.1002/2014JB011338

Szabo, B.J., and Lindsey, D.A., 1986, Estimating limiting age for Pleistocene erosional surfaces in central Montana by uranium-series dating of associated travertines: Earth Surface Processes and Landforms, v. 11, no. 2, p. 223–228, doi: https://doi.org/10.1002/esp.3290110212

USGS, 2006, Quaternary fault and fold database for the United States: https://earthquake.usgs.gov/hazards/qfaults/ [Accessed December 8, 2017]

Vergnolle, M., Pollitz, F., and Calais, E., 2003, Constraints on the viscosity of the continental crust and mantle from GPS measurements and post-seismic deformation models in western Mongolia: Journal of Geophysical Research: Solid Earth, v. 108, no. B10, 12 p., doi: https://doi.org/10.1029/2002JB002374

Vuke, S.M., 2013, Landslide map of the Big Sky area, Madison and Gallatin Counties, Montana: Montana Bureau of Mines and Geology Open-File Report 632, scale 1:24,000.

Vuke, S.M., Porter, K.W., Lonn, J.D., and Lopez, D.A., 2007, Geologic map of Montana: Montana Bureau of Mines and Geology Geologic Map 62, scale 1:500,000.

Vuke, S.M., and Stickney, M.C., 2013, Geologic map of the Clarkston Valley, Broadwater and Gallatin Counties, west-central Montana: Montana Bureau of Mines and Geology Open-File Report 642, scale 1:24,000.

Waite, G.P., and Smith, R.B., 2004, Seismotectonics and stress field of the Yellowstone volcanic plateau from earthquake first-motions and other indicators: Journal of Geophysical Research: Solid Earth, v. 109, no. B2, 14 p., doi: https://doi.org/10.1029/2003JB002675

Wang, L., Wang, R., Roth, F., Enescu, B., Hainzl, S., and Ergintav, S., 2009, Afterslip and viscoelastic relaxation following the 1999 M 7.4 İzmit earthquake from GPS measurements: Geophysical Journal International, v. 178, no. 3, p. 1220–1237, doi: https://doi.org/10.1111/j.1365-246X.2009.04228.x

Wegmann, K.W., Zurek, B.D., Regalla, C.A., Bilardello, D., Wollenberg, J.L., Kopczynski, S.E., Ziemann, J.M., Haight, S.L., Apgar, J.D., Zhao, C., and Pazzaglia, F.J., 2007, Position of the Snake River watershed divide as an indicator of geodynamic processes in the greater Yellowstone region, western North America: Geosphere, v. 3, no. 4, p. 272–281, doi: https://doi.org/10.1130/GES00083.1

Whipple, K.X., DiBiase, R.A., Ouimet, W.B., and Forte, A.M., 2017, Preservation or piracy: Diagnosing low-relief, high-elevation surface formation mechanisms: Geology, v. 45, no. 1, p. 91-94, doi: https://doi.org/10.1130/G38490.1

White, B.J.P., Smith, R.B., Husen, S., Farrell, J.M., and Wong, I., 2009, Seismicity and earthquake hazard analysis of the Teton-Yellowstone region, Wyoming: Journal of Volcanology and Geothermal Research, v. 188, no. 1–3, p. 277–296, doi: https://doi.org/10.1016/j.jvolgeores.2009.08.015

Witkind, I.J., 1964, Reactivated faults north of Hebgen Lake: U.S. Geological Survey Professional Paper, v. 435–G, p. 37–50.

Wong, I., Olig, S.S., Dober, M., Wright, D., Nemser, E., Lageson, D.R., Silva, W., Stickney, M.C., Lemieux, M., and Anderson, L., 2005, Probabilistic earthquake hazard maps for the State of Montana: Montana Bureau of Mines and Geology Special Publication 117, 72 p.

Wong, I.G., Olig, S.S., Gorton, A.E., and Naugler, W.E., 1999, Seismotectonic evaluation of the Broadwater Power Project, Toston Dam, Montana: Unpublished final report prepared for Montana Department of Natural Resources and Conservation.

Yang, R., Willett, S.D., and Goren, L., 2015, In situ low-relief landscape formation as a result of river network disruption: Nature, v. 520, no. 7548, p. 526–529.

Zoback, M.L., and Zoback, M., 1980, State of stress in the conterminous United States: Journal of Geophysical Research: Solid Earth, v. 85, no. B11, p. 6113–6156, doi: https://doi.org/10.1029/JB085iB11p06113

Zreda, M., and Noller, J.S., 1998, Ages of prehistoric earthquakes revealed by cosmogenic chlorine-36 in a bedrock fault scarp at Hebgen Lake: Science, v. 282, no. 5391, p. 1097–1099, doi: https://doi.org/10.1126/science.282.5391.1097